

Table 4 Summary of the genes located on the neighboring region of 2p15-p16.1 microdeletions

Symbol	Gene name	Location†	RefSeq Summary
<i>BCL11A</i>	B-cell CLL/lymphoma 11A	chr2:60,684,329-60,780,633	The corresponding mouse gene may function as a leukemia disease gene.
<i>PAPOLG</i>	poly(A) polymerase gamma	chr2:60,983,365-61,029,221	This gene encodes a member of the poly(A) polymerase family.
<i>REL</i>	v-rel reticuloendotheliosis viral oncogene homolog	chr2:61,108,752-61,150,178	Mutation or amplification of this gene is associated with B-cell lymphomas.
<i>PUS10</i>	pseudouridylate synthase 10	chr2:61,167,548-61,244,328	Function as the most common posttranscriptional nucleotide modification found in RNA.
<i>PEX13</i>	peroxisomal biogenesis factor 13	chr2:61,244,812-61,279,125	Related to peroxisome biogenesis disorder 11A (Zellweger).
<i>KIAA1841</i>		chr2:61,293,363-61,365,169	N/A
<i>AHSA2</i>	AHA1, activator of heat shock 90 kDa protein ATPase homolog 2	chr2:61,404,553-61,414,686	N/A
<i>USP34</i>	ubiquitin specific peptidase 34	chr2:61,414,590-61,697,849	N/A
<i>XPO1</i>	exportin 1	chr2:61,705,069-61,765,369	This cell-cycle-regulated gene encodes a protein that mediates leucine-rich nuclear export signal (NES)-dependent protein transport.
<i>FAM161A</i>	family with sequence similarity 161	chr2:62,051,983-62,081,278	Mutations in this gene cause autosomal recessive retinitis pigmentosa-28.
<i>CCT4</i>	chaperonin containing TCP1, subunit 4	chr2:62,095,262-62,115,806	The chaperonin containing the TCP1 ring complex.
<i>COMMD1</i>	copper metabolism (Murr1) domain containing 1	chr2:62,132,803-62,363,205	A regulator of copper homeostasis, sodium uptake, and NF-kappa-B signaling.
<i>B3GNT2</i>	UDP-GlcNAc:betaGal beta-1,3-N-acetylglucosaminyltransferase 2	chr2:62,423,262-62,451,866	This encodes a member of the beta-1,3-N-acetylglucosaminyltransferase family.
<i>TMEM17</i>	transmembrane protein 17	chr2:62,727,356-62,733,604	N/A
<i>EHBP1</i>	EH domain binding protein 1	chr2:62,900,986-63,273,621	The encoded protein may play a role in endocytic trafficking.

†Genomic locations are referred to build19. N/A, not available.

functional relevance of *XPO1* haploinsufficiency to the neurological features of 2p15-p16.1 microdeletion syndrome is unclear.

USP34 and *XPO1* have functional relevance to cancer, but roles for these genes in neurological functions have not been reported. We checked the Human Genetic Variation Browser (HGVB, <http://www.genome.med.kyoto-u.ac.jp/SnpDB>) to determine whether gene variants leading to loss-of-function had been reported. However, there were no such variants in the regions of *USP34* and *XPO1*.

The region neighboring the 2p15-p16.1 microdeletion does not include genes with relevance to neurological functions (Table 4), and the genes responsible for the neurological features of 2p15-p16.1 microdeletion syndrome are unknown. Diagnosis of additional patients with 2p15-p16.1 microdeletion syndrome and

identification of pathogenic mutations in the 2p15-p16.1 region will help elucidate genes that contribute to the neurological features of this syndrome.

ACKNOWLEDGMENTS

We would like to express our gratitude to the patients and their families for their cooperation. This work was mainly supported by a grant from the Precursory Research for Embryonic Science and Technology (PRESTO), Japan Science and Technology Agency (JST), Kawaguchi, Japan and was partially supported by a Grant-in-Aid for Young Scientists (B) (24791090), from the Japan Society for the Promotion of Science (JSPS), a grant from the Japan

Epilepsy Research Foundation (JERF), and a grant from the Kanae Foundation for the promotion of Medical Science in Japan (KS), and a Grant-in-Aid for Scientific Research from Health Labor Sciences Research Grants from the Ministry of Health, Labor, and Welfare, Japan (TY).

DISCLOSURES

None.

REFERENCES

- Chabchoub E, Vermeesch JR, de Ravel T et al. 2008. The facial dysmorphism in the newly recognised microdeletion 2p15-p16.1 refined to a 570 kb region in 2p15. *J Med Genet* 45:189–192.
- de Leeuw N, Pfundt R, Koolen DA et al. 2008. A newly recognised microdeletion syndrome involving 2p15p16.1: narrowing down the critical region by adding another patient detected by genome wide tiling path array comparative genomic hybridisation analysis. *J Med Genet* 45:122–124.
- Emanuel BS, Shaikh TH. 2001. Segmental duplications: an “expanding” role in genomic instability and disease. *Nat Rev Genet* 2:791–800.
- Fannemel M, Baroy T, Holmgren A et al. 2014. Haploinsufficiency of XPO1 and USP34 by a de novo 230 kb deletion in 2p15, in a patient with mild intellectual disability and cranio-facial dysmorphisms. *Eur J Med Genet* 57:513–519.
- Felix TM, Petrin AL, Sanseverino MT et al. 2010. Further characterization of microdeletion syndrome involving 2p15-p16.1. *Am J Med Genet A* 152A:2604–2608.
- Florisson JM, Mathijssen IM, Dumeé B et al. 2013. Complex craniosynostosis is associated with the 2p15p16.1 microdeletion syndrome. *Am J Med Genet A* 161A:244–253.
- Hancarova M, Simandlova M, Drabova J et al. 2013. A patient with de novo 0.45 Mb deletion of 2p16.1: the role of BCL11A, PAPOLG, REL, and FLJ16341 in the 2p15-p16.1 microdeletion syndrome. *Am J Med Genet A* 161A:865–870.
- Huchtagowder V, Liu TC, Paciorkowski AR et al. 2012. Chromosome 2p15p16.1 microdeletion syndrome: 2.5 Mb deletion in a patient with renal anomalies, intractable seizures and a choledochal cyst. *Eur J Med Genet* 55:485–489.
- Jorgez CJ, Rosenfeld JA, Wilken NR et al. 2014. Genitourinary defects associated with genomic deletions in 2p15 encompassing OTX1. *PLoS ONE* 9:e107028.
- Kau TR, Silver PA. 2003. Nuclear transport as a target for cell growth. *Drug Discov Today* 8:78–85.
- Kleinjan DA, van Heyningen V. 2005. Long-range control of gene expression: emerging mechanisms and disruption in disease. *Am J Hum Genet* 76:8–32.
- Liang JS, Shimojima K, Ohno K et al. 2009. A newly recognised microdeletion syndrome of 2p15-16.1 manifesting moderate developmental delay, autistic behaviour, short stature, microcephaly, and dysmorphic features: a new patient with 3.2 Mb deletion. *J Med Genet* 46:645–647.
- Lui TT, Lacroix C, Ahmed SM et al. 2011. The ubiquitin-specific protease USP34 regulates axin stability and Wnt/beta-catenin signaling. *Mol Cell Biol* 31:2053–2065.
- Muqbil I, Kauffman M, Shacham S et al. 2014. Understanding XPO1 target networks using systems biology and mathematical modeling. *Curr Pharm Des* 20:56–65.
- Navado J, Mergener R, Palomares-Bralo M et al. 2014. New microdeletion and microduplication syndromes: a comprehensive review. *Genet Mol Biol* 37:210–219.
- Piccione M, Piro E, Serraino F et al. 2012. Interstitial deletion of chromosome 2p15-16.1: report of two patients and critical review of current genotype-phenotype correlation. *Eur J Med Genet* 55:238–244.
- Prontera P, Bernardini L, Stangoni G et al. 2011. Deletion 2p15-16.1 syndrome: case report and review. *Am J Med Genet A* 155A:2473–2478.
- Raices M, D’Angelo MA. 2012. Nuclear pore complex composition: a new regulator of tissue-specific and developmental functions. *Nat Rev Mol Cell Biol* 13:687–699.
- Rajcan-Separovic E, Harvard C, Liu X et al. 2007. Clinical and molecular cytogenetic characterisation of a newly recognised microdeletion syndrome involving 2p15-16.1. *J Med Genet* 44:269–276.
- Shimojima K, Okamoto N, Suzuki Y et al. 2012. Subtelomeric deletions of 1q43q44 and severe brain impairment associated with delayed myelination. *J Hum Genet* 57:593–600.
- Stankiewicz P, Lupski JR. 2002. Molecular-evolutionary mechanisms for genomic disorders. *Curr Opin Genet Dev* 12:312–319.
- Williams SR, Aldred MA, Der Kaloustian VM et al. 2010. Haploinsufficiency of HDAC4 causes brachydactyly mental retardation syndrome, with brachydactyly type E, developmental delays, and behavioral problems. *Am J Hum Genet* 87:219–228.
- Wohlleber E, Kirchhoff M, Zink AM et al. 2011. Clinical and molecular characterization of two patients with overlapping de novo microdeletions in 2p14-p15 and mild mental retardation. *Eur J Med Genet* 54:67–72.

An Association of 19p13.2 Microdeletions With Malan Syndrome and Chiari Malformation

Keiko Shimojima,^{1,2} Nobuhiko Okamoto,³ Akiko Tamasaki,⁴ Noriko Sangu,^{2,5} Shino Shimada,^{2,6} and Toshiyuki Yamamoto^{2*}

¹Precursory Research for Embryonic Science and Technology (PRESTO), Japan Science and Technology Agency (JST), Kawaguchi, Japan

²Tokyo Women's Medical University Institute for Integrated Medical Sciences, Tokyo, Japan

³Department of Medical Genetics, Osaka Medical Center and Research Institute for Maternal and Child Health, Osaka, Japan

⁴Division of Child Neurology, Tottori University, Tottori, Japan

⁵Department of Dental surgery, Tokyo Women's Medical University, Tokyo, Japan

⁶Department of Pediatrics, Tokyo Women's Medical University, Tokyo, Japan

Manuscript Received: 29 April 2014; Manuscript Accepted: 12 December 2014

Patients with microdeletions in the 19p13.2 chromosomal region show developmental delays, overgrowth, and distinctive features with big head appearances. These manifestations are now recognized as Sotos syndrome-like features (Sotos syndrome 2) or Malan syndrome. We identified three female patients with 19p13.2 deletions involving *NFIX*, a gene responsible for Malan syndrome. We compared the genotypic and phenotypic data of these patients with those of the patients previously reported. The most of the clinical features were found to overlap; however, Chiari malformation type I was observed in two of the three patients evaluated in this study. Because Chiari malformation type I has never been reported in the patients with *NSD1*-related Sotos syndrome, this finding indicates the possible role of 19p13.2 deletion in patients with mimicking features of Sotos syndrome but have negative *NSD1* testing results.

© 2015 Wiley Periodicals, Inc.

Key words: 19p13.2 microdeletion; developmental delay; Sotos syndrome-like features (Sotos syndrome 2); Malan syndrome; Chiari malformation type I; *NFIX*

INTRODUCTION

Although chromosome 19 ranks 20th in size among 24 chromosomes in human genome (smaller than chromosome X), it has the 3rd highest number of genes, indicating that this chromosome is extremely gene-rich [Nussbaum et al., 2007]. This may explain the reason why deletions of chromosome 19 are rare. Chromosome 19 is also characterized with the absence of a distinguishable band in either arm upon G-banding; the only dark band that is distinguishable by G-banding is the centromere. For these reasons, continuous gene syndromes associated with chromosome 19 had rarely been recognized previously. After the advent of chromosomal microarray technologies, certain microdeletion syndromes of chromosome 19 have been reported because microarray technology does not require

How to Cite this Article:

Shimojima K, Okamoto N, Tamasaki A, Sangu N, Shimada S, Yamamoto T. 2015. An association of 19p13.2 microdeletions with malan syndrome and chiari malformation.

Am J Med Genet Part A 167A:724–730.

the recognition of banding patterns. Microdeletion syndrome of 19p13.2 is one of the newly identified conditions associated with chromosome 19. Since 2009, several patients have been reported to have deletions in this region [Auvin et al., 2009; Lysy et al., 2009; Bonaglia et al., 2010]. In 2010, Dolan et al. reported four patients with microdeletions involving 19p13.13 who shared a unique constellation of phenotypic features; i.e., developmental disabilities, overgrowth, macrocephaly, and ophthalmologic and gastrointestinal findings [Dolan et al., 2010]. They also discussed that deletions in this region may also be associated with patients who were initially

Grant sponsor: Precursory Research for Embryonic Science and Technology (PRESTO); Grant sponsor: Japan Science and Technology Agency (JST); Grant sponsor: Grant-in-Aid for Young Scientists; Grant number: 24791090; Grant sponsor: Japan Society for the Promotion of Science (JSPS); Grant sponsor: Japan Epilepsy Research Foundation (JERF); Grant sponsor: Kanae Foundation; Grant sponsor: Health Labor Sciences Research Grants.

*Correspondence to:

Toshiyuki Yamamoto, M.D., Ph.D., Tokyo Women's Medical University Institute for Integrated Medical Sciences, 8-1 Kawada-cho, Shinjuku-ward, Tokyo 162-8666, Japan.

E-mail: yamamoto.toshiyuki@twmu.ac.jp

Article first published online in Wiley Online Library

(wileyonlinelibrary.com): 3 March 2015

DOI 10.1002/ajmg.a.36959

diagnosed with Sotos syndrome but upon subsequent testing showed no abnormalities in the nuclear receptor binding SET domain protein 1 gene (*NSD1*) testing [Dolan et al., 2010]. Because the smallest region of overlap (SRO) was narrowed down to the smallest deletion region in one of the four patients [Dolan et al., 2010], the gene responsible for such clinical features was suspected to be located in SRO. In 2010, Malan et al. identified two additional patients with small deletions that partially involved the nuclear factor I/X gene (*NFIX*). Upon screening the *NFIX* sequence in 76 patients with manifestations mimicking Sotos syndrome-like features or Marshall-Smith syndrome, a nonsense mutation was identified in a patient with Sotos syndrome-like features [Malan et al., 2010]. Therefore, *NFIX* is considered to be a gene responsible for Sotos syndrome-like features, although the functional linkage between *NFIX* and *NSD1* has never been revealed. Malan et al. [2010] used the term “Sotos syndrome-like features” for the patients with overgrowth and the distinct facial features similar to the patients with *NSD1* related Sotos syndrome; i.e., a prominent forehead, high anterior hairline, downslanting palpebral fissures and prominent chin. At present, this clinical condition is proposed to be referred to as Malan syndrome [Klaassens et al., 2014] and is classified into Sotos syndrome 2 (OMIM#614753) by Online Mendelian Inheritance in Man (<http://www.omim.org/>).

Recently, we encountered three patients with 19p13.2 deletions involving *NFIX*. Two of the three patients also showed Chiari malformation type I which has never been reported in patients with Sotos syndrome. Therefore, this complication may be a noteworthy feature of 19p13.2 deletion, and a feature distinguishing it from Sotos syndrome.

PATIENT REPORTS

Patient 1

A 5-year-old girl was born at 41 gestational weeks with a birth weight of 3,710 g (90–97th centile), a length of 52 cm (75–90th centile), and an occipito-frontal circumference (OFC) of 38.4 cm (>97th centile), indicating macrocephaly. She had a past history of febrile seizure, but an electroencephalogram (EEG) showed no definite abnormality. Developmental delay was noted from early infancy, and brain magnetic resonance imaging (MRI) examined at her age of 3 years showed a finding of Chiari malformation type I (Fig. 1).

At present, she can walk with support. Her height is 122 cm (>97th centile), and her weight is 19 kg (75–90th centile), with her OFC of 55.8 cm (>97th centile), indicating overgrowth and macrocephaly. Distinctive facial findings such as frontal bossing, sparse eyebrows, hypertelorism, downslanting palpebral fissures, low-set ears, and long philtrum are noted (Fig. 1). From these features, she was clinical diagnosed as having Sotos syndrome; however, cytogenetic testing with conventional G-banding and fluorescence in situ hybridization (FISH) analysis showed no abnormality, and direct sequencing for *NSD1* revealed no mutation.

Patient 2

A 2-year-old girl was born at 37 weeks and 2 days by an emergency Caesarian due to fetal distress. The infant showed intra-uterine

growth retardation (IUGR) with a birth weight of 2,252 g (10–50th centile), a length of 47 cm (10–50th centile), and an OFC of 32.5 cm (10–50th centile). The apgar score was 3 and 5 at 1 and 5 min, respectively. Due to respiratory failure, she required intubation and artificial respiration, and was admitted to the neonatal intensive care unit (NICU). At 26 days after birth, she was weaned from mechanical ventilation. She needed tube feeding until 8 months after birth. A delay in development during infancy prompted the examination by brain MRI at 18 months, which revealed Chiari malformation type I, mildly reduced volume of the white matter, and the thin corpus callosum (Fig. 1).

At present, her length is 81.5 cm (10–25th centile), weight is 8.7 kg (<3rd centile), and OFC is 48.6 cm (75–90th centile), indicating that her head is large in comparison to her stature. She showed frontal bossing, a flat nasal bridge, midface hypoplasia, depressed eye orbits, telecanthus, low-set ears, and a tented mouth (Fig. 1). She can roll over but could not sit up by herself. She could not speak any meaningful words. Her psychomotor development was evaluated by the Kyoto Scale of Psychological Development (KSPD) and her developmental quotient (DQ) was determined to be 20. Neurological examination revealed generalized hypotonia and reduced deep tendon reflexes. Peripheral nerve conduction velocities showed no abnormalities. Conventional G-banding and subtelomere FISH analyses showed no abnormalities.

Patient 3

A 2-year-old girl was born at 40 gestational weeks with a birth weight of 3,180 g (90–97th centile), a length of 50 cm (75–90th centile), and an OFC of 33.5 cm (50–75th centile). She had a past history of epileptic seizure, but EEG showed no epileptic activity. She showed developmental delay during early infancy, i.e. she could hold up her head at 6 months, rolled over at 9 months, sat up by herself at 10 months, and crawled at 13 months. At 11 months, brain MRI was examined and revealed no abnormality (Fig. 1).

At present, she cannot walk unaided. Her height is 87.8 cm (75–90th centile), weight is 10.4 kg (10–25th centile), and OFC is 49 cm (75–90th centile). Distinctive facial findings with frontal bossing, deep-set eye, sparse eyebrows, downslanting palpebral fissures, low nasal bridge, low-set ears, high palate, and thin hair are noted (Fig. 1). Her DQ of 45 was evaluated by KSPD. The otolaryngological and ophthalmologic tests showed no abnormalities. Conventional G-banding showed a normal female karyotype, and a targeted FISH analysis for Sotos syndrome showed no deletion.

Information of the placental weights of these three patients was unavailable.

METHODS AND RESULTS FOR GENETIC TESTING

This study was approved by the ethical committee of Tokyo Women's Medical University. After obtaining the written informed consent from the patients' families, chromosomal microarray testing was performed on the three patients by using the Agilent array (Agilent Technologies, Santa Clara, CA) as described previously [Shimojima et al., 2011]. After obtaining the patients' peripheral blood samples, DNA was extracted by the QIAamp DNA extraction kit (QIAGEN, Hilden, Germany). Metaphase spreads

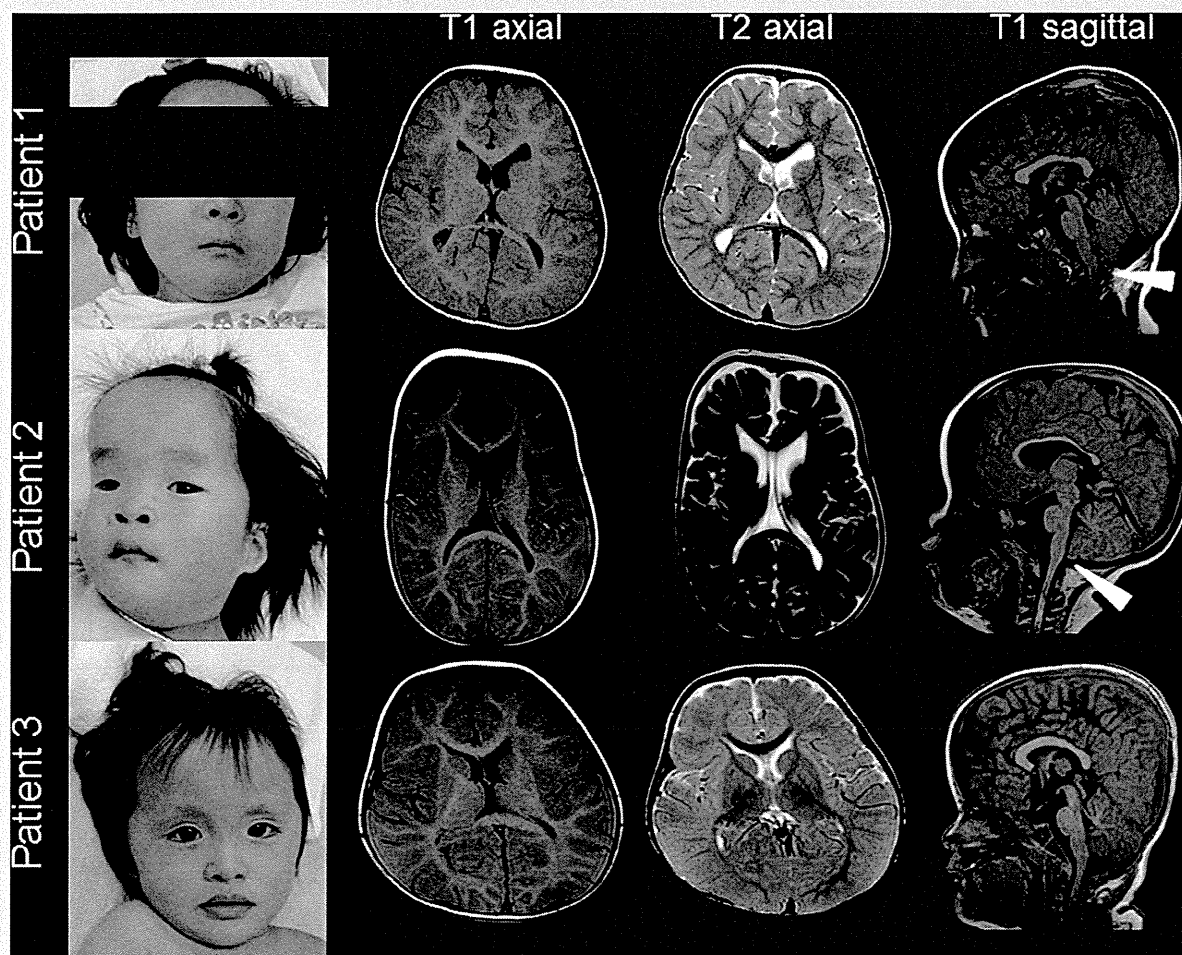


FIG. 1. Distinctive features and brain MRI findings of the patients evaluated in this study. All patients show frontal bossing, sparse eyebrows, hypertelorism, downslanting palpebral fissures, and long philtrum. T1-weighted and T2-weighted axial images and T1-weighted sagittal images of the brain MRI are shown. Patients 1, 2, and 3 were 3 years, 18 months, and 11 months of age, respectively. Patients 1 and 2 show Chiari malformation type I as indicated by arrowheads.

were prepared from peripheral blood lymphocytes by using standard methods. FISH analysis was performed using human bacterial artificial chromosomes (BAC); RP11-957I1 (19p13.2:12,564,614–12,739,959) as a target probe and RP11-974H20 (19q13.12:35,866,875–36,070,229) as a reference probe. Those were selected from the UCSC genome browser (<http://www.genome.ucsc.edu>) (GRCh37/hg19). All of the genomic positions refer to build19 in this study.

Genomic copy number losses were identified at the 19p13.2 region in all three patients; arr 19p13.2-p13.12(12,601,112–13,865,390) × 1 (Patient 1), arr 19p13.2(12,721,305–14,485,846) × 1 (Patient 2), and arr 19p13.2(12,527,157–13,563,832) × 1 (Patient 3) (Fig. 2). FISH analyses confirmed the deletion in all three patients (Fig. 2). Because their parents showed no deletion in this region, all of the deletions identified in the patients were confirmed to have de novo origins. The deletions identified in the patients are depicted in the genome map and are compared with previously reported deletions (Fig. 3).

Parental origins of the deletions were analyzed by use of the Linkage Mapping Set v2.5 HD10 and GeneMapper (Life Technologies, Foster City, CA) (Supplemental Figure S1) as described previously [Shimajima et al., 2011]. D19S221 was selected since it was the only marker included in the deletion region. By this analysis, the deletion identified in patient 3 was determined to be occurred on the paternally derived allele. The result of the linkage analysis in the family of Patient 2 showed no information due to the overlapping of the marker size. Regarding Patient 1, we had only carnoy's sample for FISH analysis. Therefore, we could not analyze the parental origins of the deletions.

DISCUSSION

In this study, we identified de novo 19p13.2 deletions in three female patients. All the identified deletions included *NFIX*. The three patients in this study showed mimicking features with Sotos syndrome; i.e., the frontal bossing, deep set eyes, sparse eyebrows,

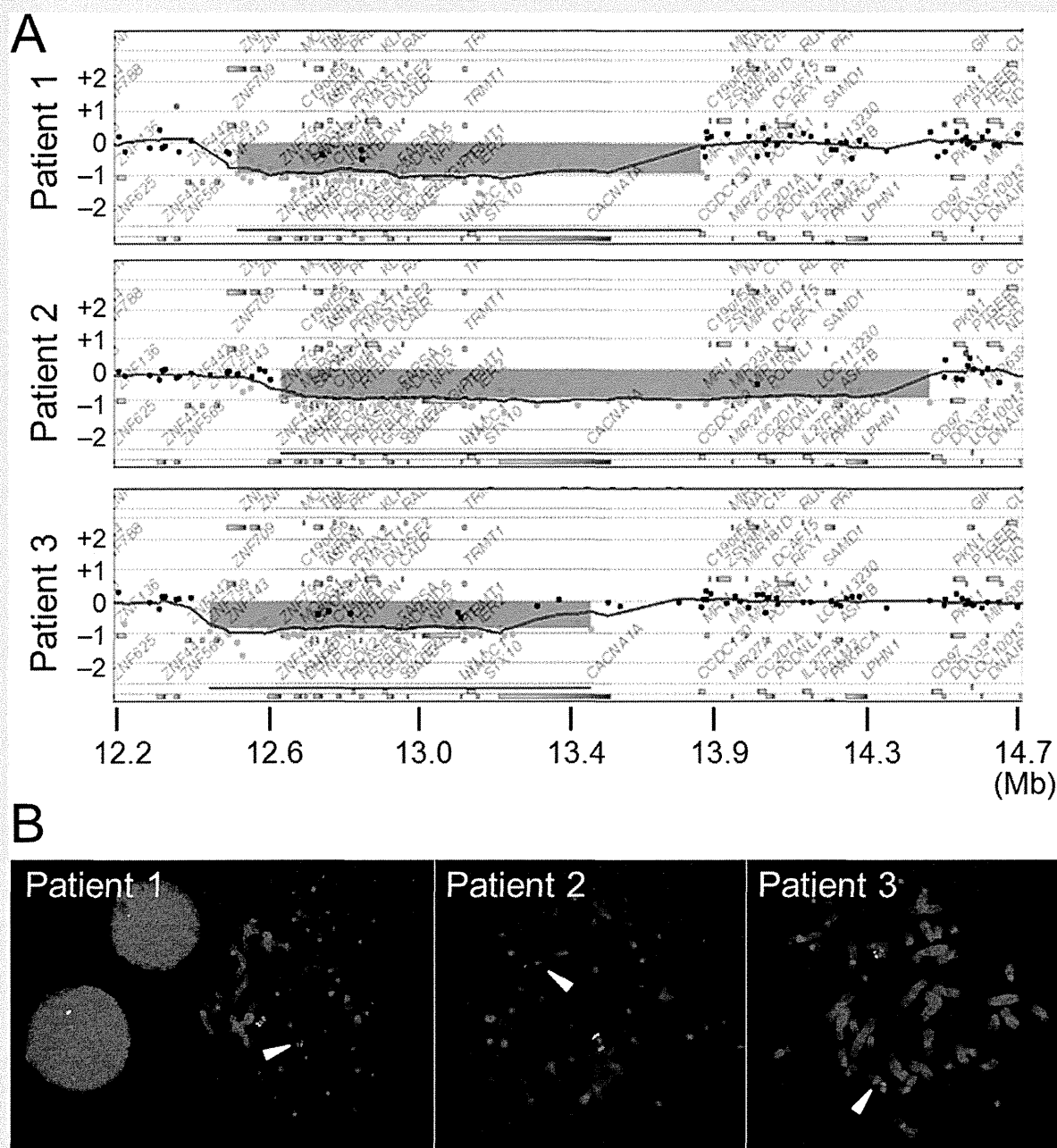


FIG. 2. The results of molecular and cytogenetic examinations. **(A):** The deletion regions are expanded by Gene View from the Agilent Genomic Workbench (Agilent Technologies). X- and Y- axes indicate genomic regions and signal \log_2 ratio, respectively. Aberrant regions are indicated by blue rectangles. Dots indicate the genomic positions and the \log_2 ratio of each probe. **(B):** Results of FISH analyses. Loss of the green signal labeled for RP11-95711 (arrow) indicates deletions of 19p13.2 in patients. Red signals are the markers of chromosome 19 labelled for RP11-974H20.

downslanting palpebral fissures, low-set ears, and low nasal bridges. Although macrocephaly was confirmed only in Patient 1, the big head appearance was also noted in Patients 2 and 3 (Fig. 1). Furthermore, all three patients were initially suspected as having Sotos syndrome owing to these clinical features. Previously, 16 patients with 19p13.2 deletions including *NFIX* have been reported

[Auvin et al., 2009; Lysy et al., 2009; Bonaglia et al., 2010; Dolan et al., 2010; Malan et al., 2010; Nimmakayalu et al., 2013; Klaassens et al., 2014; Natiq et al., 2014] (Fig. 3). All patients other than Patient 3 reported by Bonaglia et al. [2010] were either macrocephalic or relative macrocephalic with frontal bossing. Therefore, macrocephaly or a big head appearance resembling Sotos syndrome would

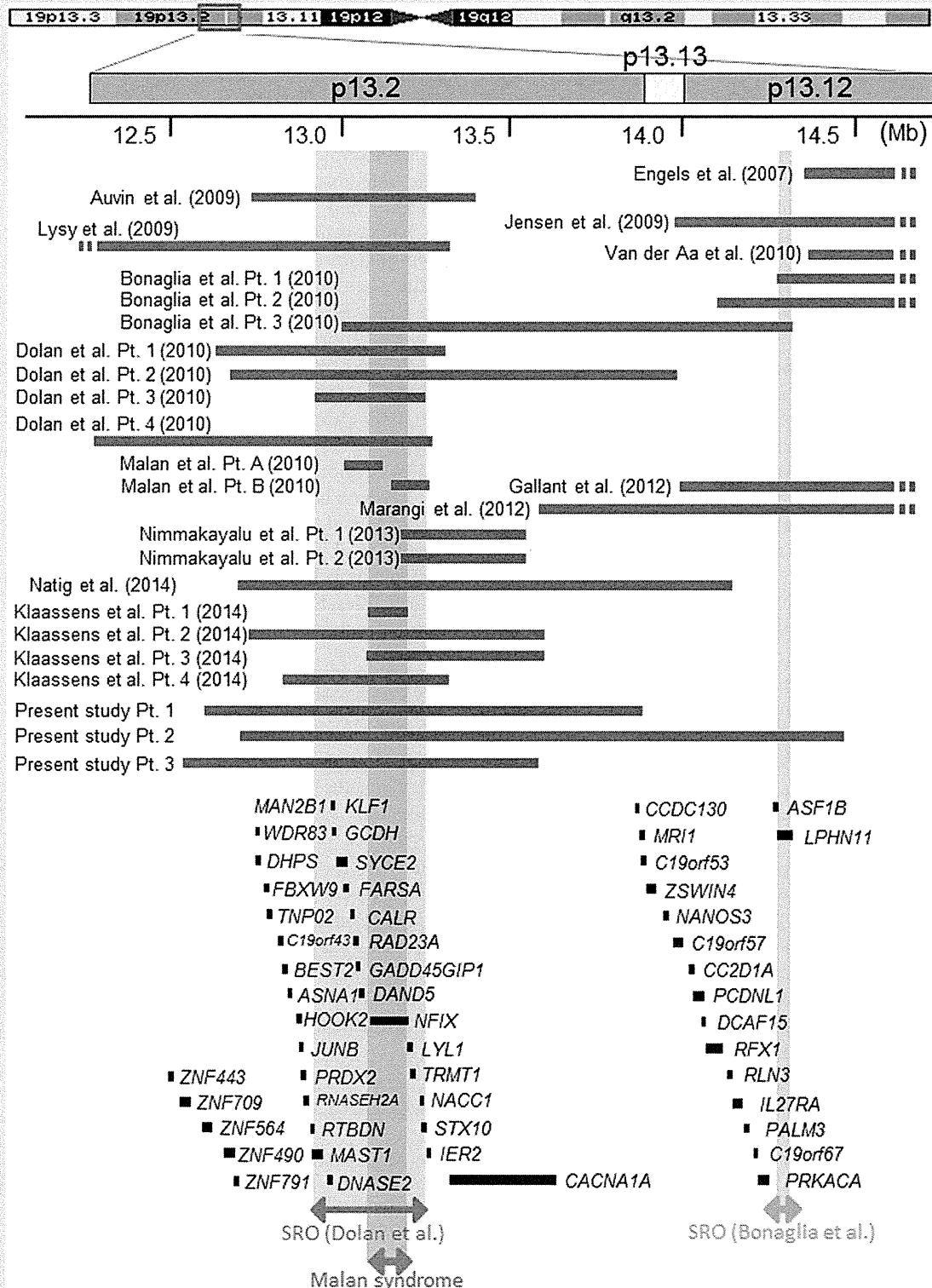


FIG. 3. Genome map of 19p13.2-p13.12 region depicting previously reported deletions. The red rectangles indicate the regions deleted in the patients evaluated in previous reports. Directions of the pointed trapezoids indicate continuous deletions. The black rectangles indicate the locations of the known genes. The SRO proposed by Dolan et al. [2010] and Bonaglia et al. [2010] are shown by bars with arrowhead on both sides. Malan syndrome critical region [NFIX region] is also shown by a bar with arrowhead on both sides. Pt, patient.

be characteristic of patients with 19p13.2 deletions or Malan syndrome.

Malan et al. [2010] identified frameshift and donor-splice site mutations of *NFIX* in patients with Marshall-Smith syndrome (OMIM#602535), another overgrowth syndrome with osteochondrodysplasia characterized by an accelerated skeletal maturation, relative postnatal failure to thrive, respiratory difficulties, mental retardation, and unusual facial features [Adam et al., 2005]. It is suggested that the dominant-negative effects of the truncated *NFIX* protein may cause Marshall-Smith syndrome [Malan et al., 2010]. Compared to that, *NFIX* missense mutations identified in two patients reported by Yoneda et al. [2012] were proposed to result in the loss of transcriptional regulation by the *NFIX* protein resulting in a Sotos syndrome-like features (Malan syndrome). Priolo et al. [2012] also reported another patient who showed the clinical features of a Sotos syndrome-like feature and had a small in-frame deletion in the N-terminal portion of the *NFIX* protein. All of the six patients reported by Klaassens et al. [2014] showed clinical features of Malan syndrome; four showed 19p13.2 deletion including *NFIX* and two showed sequencing variants of *NFIX* leading to null function. From these reports, it is suggested that the haploinsufficiency or loss-of-function mutation of *NFIX* are related to Sotos syndrome-like features (Malan syndrome).

In this study, two of the three patients had Chiari malformation type I, which has never been reported in patients with Sotos syndrome. Patient 4 reported by Dolan et al. [2010] also showed Chiari malformation type I, indicating the incidence of this finding in patients with 19p13.2 deletions involving *NFIX* is 3/19 (15.8%). Because Chiari malformation type I is a heterogeneous syndrome, identifications of this finding may be just coincidental. However, if the combination between 19p13.2 deletions and Chiari malformation type I was a specific finding, the presence of Chiari malformation type I may help differentiate the 19p13.2 deletion syndrome from the Sotos syndrome related to *NSD1*. One of the explanations is that allelic loss of *NFIX* per se may be related to Chiari malformation type I, because *NFIX* has a role in the regulation of cerebellar development [Piper et al., 2011]. Alternatively, the neighboring genes to *NFIX* may be related to this. The deletion regions of 19p13.2, identified in patients manifesting both of Sotos syndrome-like features and Chiari malformation type I, included some other neighboring genes that are expressed in the brain and neural tissues, and represent candidate genes for clinical manifestations. The microtubule associated serine/threonine kinase 1 gene (*MAST1*), located telomeric to *NFIX* (Fig. 3), belongs to a member of a family of microtubule-associated serine/threonine kinase genes that are highly expressed in the brain [Dolan et al., 2010]. Thus, *MAST1*, which is within the deleted region of 19p13.2 in both Patients 1 and 2 displaying Chiari malformation type I, may be related to such additional brain malformations with low penetrance because only the small number of the patients with 19p13.2 deletions showed this finding.

The second common clinical manifestation described Dolan et al. involves ophthalmologic abnormalities (particularly strabismus) and optic nerve atrophy or hypoplasia, the latter being detected by formal ophthalmologic examination and/or MRI [Dolan et al., 2010]. The third finding in this triad is gastrointestinal symptoms, particularly abdominal pain and vomiting. Klaassens et al. [2014]

reported skeletal abnormalities as recurrent complications. However, the three patients in this study did not show such clinical findings.

The calcium channel alpha 1 A subunit gene (*CACNA1A*) encodes the Cav2.1 domain, a pore-forming and voltage-sensing subunit of a neuronal P/Q type calcium channel, and is expressed throughout the central nervous system [Mori et al., 1991]. *CACNA1A* have been related to episodic ataxia type 2 (OMIM #108500), familial hemiplegic migraine 1 (OMIM #141500), familial hemiplegic migraine 1 with progressive cerebellar ataxia (OMIM #141500), and spinocerebellar ataxia 6 (OMIM #183086). In fact, haploinsufficiency of *CACNA1A* has been suggested to be responsible for epilepsy and infantile spasms in a patient reported by Auvin et al. [2009] and Patients 1 and 3 evaluated in this study have had a history of seizures. Episodic ataxia was observed in Patient 1 reported by Ninmakayalu et al. [2013]; however, the patients reported by Dolan et al. [2010] and the three patients in this study had never experienced episodes of ataxia, suggesting low phenotypic penetrance of the dosage-effects of *CACNA1A*.

Patient 2 in this study showed a larger deletion involving 19p13.12 region (Fig. 3); several patients with deletions involving 19p13.12 have been reported [Engels et al., 2007; Jensen et al., 2009; Van der Aa et al., 2010; Gallant et al., 2011; Marangi et al., 2012], and Bonaglia et al. [2010] proposed the SRO that is responsible for developmental delay, bilateral hearing impairments and behavioral abnormalities. However, such additional phenotypic features have never been observed in Patient 2 in this study.

ACKNOWLEDGMENTS

We would like to express our gratitude to the patients and their families for their cooperation. This work was mainly supported by a grant from the Precursory Research for Embryonic Science and Technology (PRESTO) grant, from the Japan Science and Technology Agency (JST), Kawaguchi, Japan and was partially supported by a Grant-in-Aid for Young Scientists (B) (24791090), from the Japan Society for the Promotion of Science (JSPS), a grant from the Japan Epilepsy Research Foundation (JERF), and a grant from the Kanae Foundation for the promotion of Medical Science in Japan (KS). This study was partially supported by a Grant-in-Aid for Scientific Research from Health Labor Sciences Research Grants from the Ministry of Health, Labor, and Welfare, Japan (TY).

REFERENCES

- Adam MP, Hennekam RC, Keppen LD, Bull MJ, Clericuzio CL, Burke LW, Ormond KE, Hoyme EH. 2005. Marshall-Smith syndrome: Natural history and evidence of an osteochondrodysplasia with connective tissue abnormalities. *Am J Med Genet Part A* 137A:117–124.
- Auvin S, Holder-Espinasse M, Lamblin MD, Andrieux J. 2009. Array-CGH detection of a de novo 0.7-Mb deletion in 19p13.13 including *CACNA1A* associated with mental retardation and epilepsy with infantile spasms. *Epilepsia* 50:2501–2503.
- Bonaglia MC, Marelli S, Novara F, Commodaro S, Borgatti R, Minardo G, Memo L, Mangold E, Beri S, Zucca C, Brambilla D, Molteni M, Giorda R, Weber RG, Zuffardi O. 2010. Genotype-phenotype relationship in three cases with overlapping 19p13.12 microdeletions. *Eur J Hum Genet* 18:1302–1309.

- Dolan M, Mendelsohn NJ, Pierpont ME, Schimmenti LA, Berry SA, Hirsch B. 2010. A novel microdeletion/microduplication syndrome of 19p13.13. *Genet Med* 12:503–511.
- Engels H, Brockschmidt A, Hoischen A, Landwehr C, Bosse K, Walldorf C, Toedt G, Radlwimmer B, Propping P, Lichter P, Weber RG. 2007. DNA microarray analysis identifies candidate regions and genes in unexplained mental retardation. *Neurology* 68:743–750.
- Gallant NM, Baldwin E, Salamon N, Dipple KM, Quintero-Rivera F. 2011. Pontocerebellar hypoplasia in association with de novo 19p13.11p13.12 microdeletion. *Am J Med Genet Part A* 155A:2871–2878.
- Jensen DR, Martin DM, Gebarski S, Sahoo T, Brundage EK, Chinault AC, Otto EA, Chaki M, Hildebrandt F, Cheung SW, Lesperance MM. 2009. A novel chromosome 19p13.12 deletion in a child with multiple congenital anomalies. *Am J Med Genet Part A* 149A:396–402.
- Klaassens M, Morrogh D, Rosser EM, Jaffer F, Vreeburg M, Bok LA, Segboer T, van Belzen M, Quinlivan RM, Kumar A, Hurst JA, Scott RH. 2014. Malan syndrome: Sotos-like overgrowth with de novo NFIX sequence variants and deletions in six new patients and a review of the literature. *Eur J Hum Genet* 10.1038/ejhg.2014.162. [Epub ahead of print].
- Lysy PA, Ravoet M, Wustefeld S, Bernard P, Nassogne MC, Wyns E, Sibille C. 2009. A new case of syndromic craniosynostosis with cryptic 19p13.2-p13.13 deletion. *Am J Med Genet Part A* 149A:2564–2568.
- Malan V, Rajan D, Thomas S, Shaw AC, Louis D, Picard H, Layet V, Till M, van Haeringen A, Mortier G, Nampoothiri S, Puseljic S, Legeai-Mallet L, Carter NP, Vekemans M, Munnich A, Hennekam RC, Colleaux L, Cormier-Daire V. 2010. Distinct effects of allelic NFIX mutations on nonsense-mediated mRNA decay engender either a Sotos-like or a Marshall-Smith syndrome. *Am J Hum Genet* 87:189–198.
- Marangi G, Orteschi D, Vigeveno F, Felie J, Walsh CA, Manzini MC, Neri G. 2012. Expanding the spectrum of rearrangements involving chromosome 19: A mild phenotype associated with a 19p13.12-p13.13 deletion. *Am J Med Genet Part A* 158A:888–893.
- Mori Y, Friedrich T, Kim MS, Mikami A, Nakai J, Ruth P, Bosse E, Hofmann F, Flockerzi V, Furuichi T, Mikoshiba K, Imoto K, Tanabe T, Numa S. 1991. Primary structure and functional expression from complementary DNA of a brain calcium channel. *Nature* 350:398–402.
- Natiq A, Elalaoui SC, Miesch S, Bonnet C, Jonveaux P, Amzazi S, Sefiani A. 2014. A new case of de novo 19p13.2p13.12 deletion in a girl with overgrowth and severe developmental delay. *Mol Cytogenet* 7:40.
- Nimmakayalu M, Horton VK, Darbro B, Patil SR, Alsayouf H, Keppler-Noreuil K, Shchelochkov OA. 2013. Apparent germline mosaicism for a novel 19p13.13 deletion disrupting NFIX and CACNA1A. *Am J Med Genet Part A* 161A:1105–1109.
- Nussbaum R, McInnes RR, Willard HF. editors. 2007. *Thompson & Thompson Genetics in Medicine*. Philadelphia: Saunders. p600.
- Piper M, Harris L, Barry G, Heng YH, Plachez C, Gronostajski RM, Richards LJ. 2011. Nuclear factor one X regulates the development of multiple cellular populations in the postnatal cerebellum. *J Comp Neurol Part A* 519A:3532–3548.
- Priolo M, Grosso E, Mammi C, Labate C, Naretto VG, Vacalebri C, Caridi P, Lagana C. 2012. A peculiar mutation in the DNA-binding/dimerization domain of NFIX causes Sotos-like overgrowth syndrome: a new case. *Gene Part A* 511A:103–105.
- Shimajima K, Isidor B, Le Caignec C, Kondo A, Sakata S, Ohno K, Yamamoto T. 2011. A new microdeletion syndrome of 5q31.3 characterized by severe developmental delays, distinctive facial features, and delayed myelination. *Am J Med Genet Part A* 155A:732–736.
- Van der Aa N, Vandeweyer G, Kooy RF. 2010. A boy with mental retardation, obesity and hypertrichosis caused by a microdeletion of 19p13.12. *Eur J Med Genet* 53:291–293.
- Yoneda Y, Saito H, Touyama M, Makita Y, Miyamoto A, Hamada K, Kurotaki N, Tomita H, Nishiyama K, Tsurusaki Y, Doi H, Miyake N, Ogata K, Naritomi K, Matsumoto N. 2012. Missense mutations in the DNA-binding/dimerization domain of NFIX cause Sotos-like features. *J Hum Genet* 57:207–211.

SUPPORTING INFORMATION

Additional supporting information may be found in the online version of this article at the publisher's web-site.

Epilepsy in 1p36 Deletion Syndrome Is Not Associated with Deletion Size

Toshiyuki Yamamoto¹ Shino Shimada^{1,2} Keiko Shimojima¹ Hiroko Ikeda³ Kazuhiro Oguni²

¹Tokyo Women's Medical University Institute for Integrated Medical Sciences, Tokyo, Japan

²Department of Pediatrics, Tokyo Women's Medical University, Tokyo, Japan

³Department of Pediatrics, National Center for Epilepsy, Shizuoka, Japan

Address for correspondence Toshiyuki Yamamoto, MD, PhD, Tokyo Women's Medical University Institute for Integrated Medical Sciences, 8-1 Kawada-cho, Shinjuku-ward, Tokyo 162-8666, Japan (e-mail: yamamoto.toshiyuki@twmu.ac.jp).

J Pediatr Epilepsy 2015;4:4–7.

Abstract

1p36 deletion syndrome is the most common subtelomeric deletion syndrome. The main clinical features are intellectual disability, characteristic craniofacial features, and epilepsy. Recent analysis revealed that a minimum deletion of 2.2 Mb from the telomere is essential for full manifestations of 1p36 deletion syndrome. Generally, severity of neurological symptoms in patients with 1p36 deletion syndrome correlates with the size of the deletion; however, the incidence of epilepsy does not correlate with deletion size. Some patients with minimum deletions never show symptoms of epilepsy, but there are patients who manifest intractable epilepsy, especially epileptic spasms. This evidence indicates that the responsible region for epilepsy is in the minimum deletion region, but the penetrance of epilepsy is not complete. Prognosis of brain development in patients with 1p36 deletions is related to the outcome of epilepsy treatment. Careful follow-up for infantile patients with 1p36 deletion syndrome would be recommended for early diagnosis and intervention for epilepsy.

Keywords

- ▶ 1p36 deletion syndrome
- ▶ epilepsy
- ▶ incidence
- ▶ *KCNAB2*
- ▶ *GABRD*

Introduction

1p36 deletion syndrome is the most common subtelomeric deletion syndrome, and a previous study reported that the incidence of this syndrome is approximately 1 per 50,000 to 100,000 births.^{1,2} Shapira et al³ were the first to delineate the phenotype of pure 1p36 deletion syndrome; the most common features are intellectual disability, large anterior fontanel, motor delay/hypotonia, vision and hearing problems, seizures, and growth delay. Heilstedt et al⁴ analyzed the deletion sizes in patients and identified variable patterns of chromosomal abnormalities, including pure terminal deletions, unbalanced translocations, and interstitial deletions. Although the identified deletion sizes were variable among patients, critical intervals for orofacial clefting, hypothyroidism, cardiomyopathy, hearing loss, large fontanel, and hypotonia have been identified within 2.2 to 4.0 Mb.⁴ On the other

hand, the severities of neurological features are considered to be correlated with the size of the deletion.⁵ Generally, recognition of the combination of clinical characteristics acts as a preliminary clinical diagnosis in patients with chromosomal abnormalities. The final diagnosis would then be made by genetic testing—either of conventional chromosomal analysis, fluorescence in-situ hybridization analysis, or microarray-based comparative genomic hybridization (aCGH) analysis. Previously, only the larger 1p36 deletions could be detected by conventional G-banding. Now, we can detect submicroscopic deletions by use of aCGH analysis. As a consequence, many small deletions involving the 1p36 region have been reported to date.⁶ The constellation of the recent results revealed that the minimum deletion involving approximately 1.7 to 1.9 Mb from telomere is essential for full manifestations of 1p36 deletion.⁷ All patients with deletions of over 2.2 Mb manifest developmental delay and

received
September 1, 2014
accepted
September 9, 2014

Issue Theme Epilepsy in Numerical Chromosomal Abnormalities; Guest Editor: Toshiyuki Yamamoto, MD, PhD

Copyright © 2015 by Georg Thieme Verlag KG, Stuttgart · New York

DOI <http://dx.doi.org/10.1055/s-0035-1554785>.
ISSN 2146-457X.

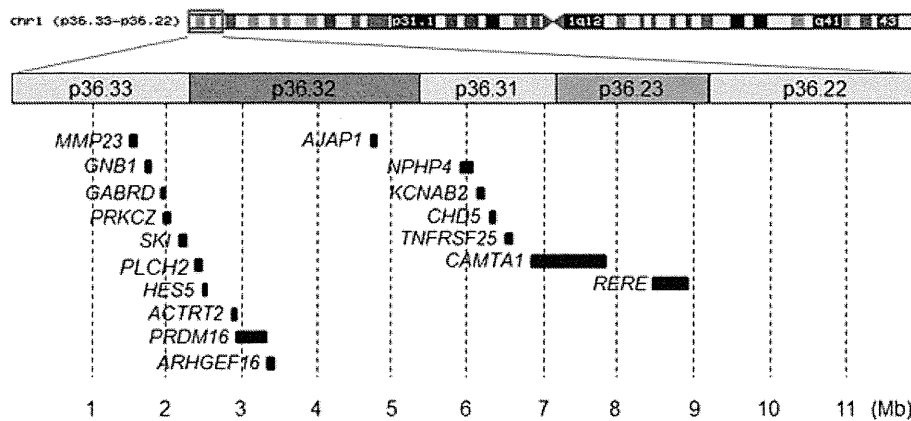


Fig. 1 The physical map of 1p36. The locations of the genes that may contribute to some clinical phenotypes in the 1p36 region are depicted, referring to the February 2009 human reference sequence (GRCh37/hg19).

characteristic craniofacial features, but the incidence rate for epilepsy is not 100%.⁸

In this review, we will discuss epilepsy in patients with 1p36 deletion syndrome.

Genes That May Contribute to Epilepsy

KCNAB2 (The Potassium Voltage-Gated Channel, Shaker-Related Subfamily, β Member 2 Gene)

KCNAB2, located on chr1:6,086,073–6,158,621 (build19), has been considered as the gene responsible for epilepsy in patients with 1p36 deletion syndrome (→**Fig. 1**); however, many patients with smaller 1p36 deletion not involving *KCNAB2* also show epilepsy. Therefore, *KCNAB2* is considered a modifier gene rather than the gene directly contributing to epilepsy. We have observed that patients with 1p36 deletion larger than 5.5 Mb do not acquire walking ability.⁹ This would indicate that there is a modifier gene for neurological prognosis around this location. Perkowski and Murphy¹⁰ analyzed *KCNAB2* knockout mice, which showed a reduction in the slow after hyperpolarization following a burst of action potentials and a concomitant increase in neuronal excitability in projection neurons in the lateral nucleus of the amygdala, suggesting a loss of function of the potassium channel, which contributes to the cognitive and neurological impairments. This supports the evidence that a *KCNAB2* deletion would be a modifier of the clinical manifestations in patients with 1p36 deletions.

GABRD (The Gamma-Aminobutyric Acid A Receptor, Delta Gene)

GABRD is located on chr1:1,950,768–1,962,192 (build19) (→**Fig. 1**). This gene encodes a ligand-gated chloride channel. A heterozygous *GABRD* mutation was identified in two affected members of a family with generalized epilepsy with febrile seizures plus.¹¹ Because the unaffected family member also carried the mutation, *GABRD* has been considered as the susceptibility gene to generalized epilepsy associated with febrile seizures, rather than the directly responsible gene. Although human variants of *GABRD* have not been identified,

GABRD is believed to be the main causative gene of epilepsy in 1p36 deletion syndrome.

Genotype–Phenotype Correlation for Epilepsy

It is believed that there is a correlation between clinical severities in patients with 1p36 deletion syndrome and the size of chromosomal deletions, which is supported by the evidence that the patients with larger deletions (>8 Mb) show severe intellectual disability and epilepsy.⁵ This suggests the existence of genetic modifiers in the proximal region of 1p36. Although the deletion of *KCNAB2* had been considered to be responsible for intractable seizures in the 1p36 deletion syndrome, this does not apply to all patients.⁵ Some patients with 1p36 deletion syndrome with small deletion (<3 Mb) show no epilepsy, and the prognosis of neurological development in such patients is better than that in patients with larger deletions. On the other hand, there are many patients with severe intractable epilepsy associated with a severe delay in development, despite the fact that the patients had deletions less than 3 Mb. In the following report, unrelated two patients will be presented.

Patient 1

A 17-month-old girl (patient 4 reported by Shimada et al⁹) was born at 40 weeks of gestation. Her birth weight was 2,540 g. There was no remarkable history during pregnancy. Her parents were healthy and nonconsanguineous, and her younger sister was also healthy. She acquired head control at 6 months; however, she did not show turning over at 9 months. She was then referred to our hospital. From her distinctive facial features, 1p36 deletion syndrome was suspected. By subtelomeric fluorescence in situ hybridization analysis, a 1p36 deletion was confirmed. Because both parents did not have a deletion, the patient's deletion was confirmed as de novo in origin. Chromosomal microarray testing revealed the deletion size as 2,239,497 bp from telomere (build19).

Just prior to turning 1 year old, she started to show head nodding. This involuntary movement was observed at an

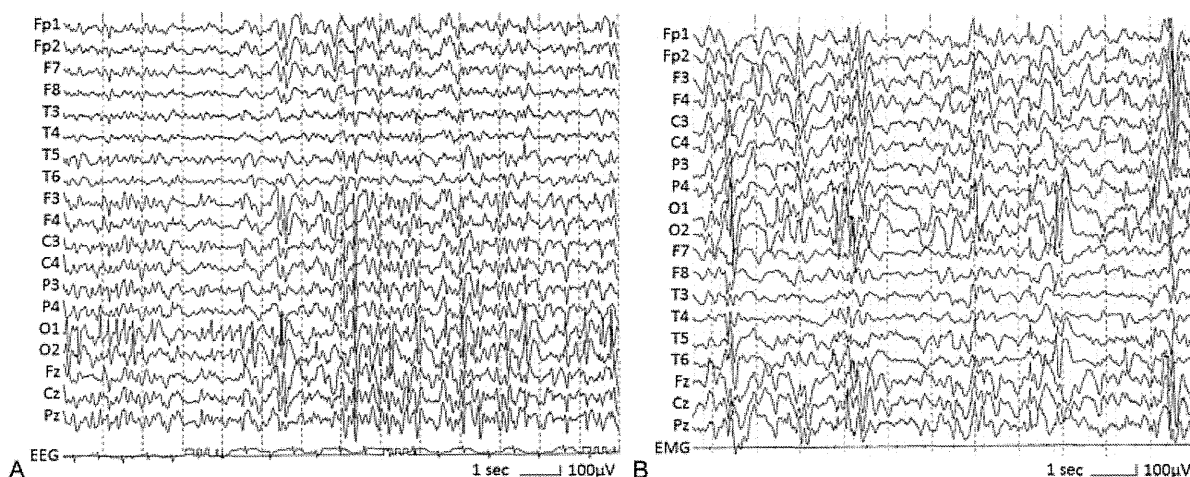


Fig. 2 Electroencephalograms of the patients with 1p36 deletion syndrome. (A) Sleep electroencephalogram of patient 1. Normal background activities are not observed. Bilateral occipital focal spikes are frequently expanded diffusely. (B) Sleep electroencephalogram in patient 2 also shows bilateral occipital focal spikes associated with diffuse theta waves. There are no normal background activities.

outpatient clinic. An electroencephalogram (EEG) was examined, and high-voltage slow waves were recorded (**Fig. 2A**). Normal background activity could not be observed. During record, a diffuse high-voltage burst with subsequent general attenuation was observed with synchronization with involuntary movements, suggesting epileptic spasms. From these findings, we diagnosed her with epileptic encephalopathy. After prescribing valproic acid, the clinical seizures were controlled.

At present, her height is 79.8 cm (+0.9 standard deviation [SD]), weight was 11.0 kg (+1.6 SD), and occipitofrontal circumference was 47.8 cm (+0.9 SD). She showed muscular hypotonia.

aCGH analysis identified a chromosomal deletion in 1p36 region with the size of 2.2 Mb. Because both parents showed no aberration, this deletion was of *de novo* origin.

Patient 2

A 7-year-old boy (patient 7 reported by Shimada et al⁹) was born with a birth weight of 3,360 g and a length of 50.5 cm. In early infancy, he showed muscular hypotonia, poor sucking, and dysphagia. When he was 1 month old, he started to show tonic-clonic seizures and he was prescribed clonazepam. It was changed to valproic acid. At the age of 8 months, a series of epileptic spasms were noted. Although clonazepam was changed into zonisamide, or nitrazepam, or topiramate, or phenobarbital, there was no effect.

When the patient was 2 years old, he was referred to our hospital. At that time, an EEG showed a continuous high-

voltage theta burst associated with spikes in the occipital region (**Fig. 2B**). Although this EEG finding did not indicate hypsarrhythmia, his clinical course was suspected as that of West syndrome. Therefore, we performed adrenocorticotrophic hormone therapy. After the second course of adrenocorticotrophic hormone therapy, his clinical seizures had disappeared.

He showed severe developmental delay, as he only developed head control and rolling over at the age of 2 years and 6 months. Now, he can sit with support, but his speech contains no meaningful words. Due to dysphagia, he requires tube feeding. An auditory examination revealed mild deafness with 50 to 90 dB. He has straight eyebrows, deep-set eyes, hypotelorism, a pointed chin, and low-set ears. Strabismus and cryptorchidism are noted, and there was no cleft lip or congenital heart defect.

aCGH analysis identified a chromosomal deletion in 1p36 region with the size of 2,553,982 bp from telomere (build19). Parental examinations were declined by his parents.

Unknown Contributors for Epilepsy

The two patients described above had smaller deletions of 2.2 and 2.6 Mb in the 1p36 region. Generally, patients with smaller deletion have a relatively good prognosis; however, these two patients showed severe epileptic encephalopathy, associated with spasms and severe EEG abnormalities. In comparison, there are many patients with 1p36 deletion syndrome who have never experienced epilepsy even if the

Table 1 Affected ratio of epilepsy in patients with 1p36 deletion syndrome

Deletion sizes (Mb)	<3	<4	<5	<6	<7	<8	<9	<10	10<
Affected number	3	7	11	12	16	19	21	23	24
Total number	5	12	16	18	22	25	31	33	35
Affected ratio	60%	58%	69%	67%	72%	86%	68%	70%	69%

Note: The patients with pure terminal deletions of 1p36 are evaluated.⁹

deletion sizes were larger than the others. In ►Table 1, the correlation between the deletion size and the affected ratio by epilepsy is shown. The subjects have been cited from our previous reports, and only the patients who showed pure terminal deletions were evaluated.⁹ As can be seen in ►Table 1, the affected ratio by epilepsy does not correlate with deletion sizes. Therefore, the manifestation of epilepsy in patients with 1p36 deletion syndrome may be modified by an unknown etiology, e.g., single nucleotide polymorphisms in the remaining allele, epigenetic factors.

Treatment for Epilepsy in Patients with 1p36 Deletion Syndrome

The clinical features of epilepsy in patients with 1p36 deletion syndrome are variable. Knight-Jones et al¹² described four patients with epilepsy associated with 1p36 deletions in details. In their study, child 1 started to have hemiconvulsions at the age of 3 months and later manifested Lennox–Gastaut syndrome. Child 2 started to show epilepsy during the first year of life and had both absence and grand mal seizures. Child 3 started to show myoclonic jerks during the second year of life. Child 4 also displayed myoclonic jerks but the manifestations resembled epileptic spasms. Saito et al¹³ reported a patient with a 1p36 deletion over 8 Mb in size who showed epileptic spasms associated with polymicrogyria. From these evidences, it is easy to understand that there are various patterns of epilepsy in patients with 1p36 deletion syndrome. Therefore, we have to thoroughly evaluate patients' epilepsy and should select a suitable treatment strategy for each patient. Consequently, there is no golden standard treatment for epilepsy in patients with 1p36 deletion syndrome. Because epileptic spasms are a poor prognostic factor, it is important to know that patients with 1p36 deletion syndrome are prone to epileptic spasms during the first year of life. Once the occurrence of epileptic spasms in patients with 1p36 deletion syndrome is observed, we should not hesitate to start a medical check-up and treatment for an improved prognosis.

In conclusion, patients with the 2.2 Mb minimum deletion of 1p36 can show severe epileptic encephalopathy, but some patients with larger deletion do not show epilepsy. This indicates that penetrance or clinical impact for epilepsy by haploinsufficiency of the gene causative for epilepsy may not be high. Therefore, the real genetic cause of epilepsy in patients with 1p36 deletion syndrome remains unknown. It is important to follow up carefully for infantile patients with 1p36 deletion syndrome, because patients with 1p36 deletions frequently show epileptic spasms.

Acknowledgments

We would like to acknowledge the Collaborative Research Supporting Committee of the Japanese Society of Child Neurology (10–11) for promoting this study. This work was supported by a Grant-in-Aid for Scientific Research from Health Labor Sciences Research Grants from the Ministry of Health, Labor, and Welfare, Japan (T. Y.).

References

- 1 Heilstedt HA, Ballif BC, Howard LA, Kashork CD, Shaffer LG. Population data suggest that deletions of 1p36 are a relatively common chromosome abnormality. *Clin Genet* 2003;64(4):310–316
- 2 Shao L, Shaw CA, Lu XY, et al. Identification of chromosome abnormalities in subtelomeric regions by microarray analysis: a study of 5,380 cases. *Am J Med Genet A* 2008;146A(17):2242–2251
- 3 Shapira SK, McCaskill C, Northrup H, et al. Chromosome 1p36 deletions: the clinical phenotype and molecular characterization of a common newly delineated syndrome. *Am J Hum Genet* 1997;61(3):642–650
- 4 Heilstedt HA, Ballif BC, Howard LA, et al. Physical map of 1p36, placement of breakpoints in monosomy 1p36, and clinical characterization of the syndrome. *Am J Hum Genet* 2003;72(5):1200–1212
- 5 Kurosawa K, Kawame H, Okamoto N, et al. Epilepsy and neurological findings in 11 individuals with 1p36 deletion syndrome. *Brain Dev* 2005;27(5):378–382
- 6 Buck A, du Souich C, Boerkoel CF. Minimal genotype–phenotype correlation for small deletions within distal 1p36. *Am J Med Genet A* 2011;155A(12):3164–3169
- 7 Rosenfeld JA, Crolla JA, Tomkins S, et al. Refinement of causative genes in monosomy 1p36 through clinical and molecular cytogenetic characterization of small interstitial deletions. *Am J Med Genet A* 2010;152A(8):1951–1959
- 8 Battaglia A, Hoyme HE, Dallapiccola B, et al. Further delineation of deletion 1p36 syndrome in 60 patients: a recognizable phenotype and common cause of developmental delay and mental retardation. *Pediatrics* 2008;121(2):404–410
- 9 Shimada S, Shimojima K, Okamoto N, et al. Microarray analysis of 50 patients reveals the critical chromosomal regions responsible for 1p36 deletion syndrome-related complications. *Brain Dev* 2015;37(5):515–526
- 10 Perkowski JJ, Murphy GG. Deletion of the mouse homolog of KCNAB2, a gene linked to monosomy 1p36, results in associative memory impairments and amygdala hyperexcitability. *J Neurosci* 2011;31(1):46–54
- 11 Dibbens LM, Feng HJ, Richards MC, et al. GABRD encoding a protein for extra- or peri-synaptic GABA receptors is a susceptibility locus for generalized epilepsies. *Hum Mol Genet* 2004;13(13):1315–1319
- 12 Knight-Jones E, Knight S, Heussler H, Regan R, Flint J, Martin K. Neurodevelopmental profile of a new dysmorphic syndrome associated with submicroscopic partial deletion of 1p36.3. *Dev Med Child Neurol* 2000;42(3):201–206
- 13 Saito Y, Kubota M, Kurosawa K, et al. Polymicrogyria and infantile spasms in a patient with 1p36 deletion syndrome. *Brain Dev* 2011;33(5):437–441

Xq28 Duplications and Epilepsy: Influence of the Combinatory Duplication of *MECP2* and *GDI1*

Toshiyuki Yamamoto¹ Shino Shimada^{1,2} Keiko Shimojima¹ Kaoru Eto² Shinsaku Yoshitomi³
Keiko Yanagihara⁴ Katsumi Imai³ Hirokazu Oguni² Nobuhiko Okamoto⁵

¹ Tokyo Women's Medical University Institute for Integrated Medical Sciences, Tokyo, Japan

² Department of Pediatrics, Tokyo Women's Medical University, Tokyo, Japan

³ National Epilepsy Center, Shizuoka Institute of Epilepsy and Neurological Disorders, Shizuoka, Japan

⁴ Department of Pediatric Neurology, Osaka Medical Center and Research Institute for Maternal and Child Health, Izumi, Japan

⁵ Department of Medical Genetics, Osaka Medical Center and Research Institute for Maternal and Child Health, Izumi, Japan

Address for correspondence Toshiyuki Yamamoto, MD, PhD, Tokyo Women's Medical University Institute for Integrated Medical Sciences, 8-1 Kawada-cho, Shinjuku-ward, Tokyo 162-8666, Japan (e-mail: yamamoto.toshiyuki@twmu.ac.jp).

J Pediatr Epilepsy 2015;4:30–34.

Abstract

Xq28 duplications including the *MECP2* (Methyl-CpG-binding protein 2) cause an X-linked recessive neurodegenerative disorder that presents symptoms such as early developmental delay, progressive deterioration, and intractable epilepsy. Submicroscopic interstitial duplication in the *MECP2* region is one of the most frequently observed submicroscopic chromosomal aberrations in patients with intellectual disability. This high prevalence is derived from the genomic instability characteristic of this region due to segmental duplications that are densely located in this region, which are prone to cause nonallelic homologous recombination during meiosis. Patients with *MECP2* duplications generally begin to show epilepsy after 6 years of age. Therefore, incidence of epilepsy is high in adolescents. Although many types of seizures have been reported in patients, the most frequently observed seizure types were absence seizure and generalized tonic-clonic seizures. Because drop attacks are frequently seen, such epileptic attacks are sometimes life-threatening. We encountered a patient who showed epileptic spasms during infancy with a relatively larger duplication that encompasses *MECP2* and *GDI1* (GDP dissociation inhibitor-1). This led us to speculate that the combinatory duplication that includes *MECP2* and *GDI1* may cause severe epileptic features; however, most of the previously reported patients with combined duplications of *MECP2* and *GDI1* did not show early occurrence of epilepsy. Therefore, further information would be required to confirm if the combinatory duplication of *MECP2* and *GDI1* exerts any influence on the severity of epilepsy.

Keywords

- ▶ Xq28 duplication
- ▶ epilepsy
- ▶ intellectual disability
- ▶ *MECP2*
- ▶ *GDI1*

Introduction

In 1999, the methyl-CpG-binding protein 2 (*MECP2*) gene located on chromosome Xq28 was identified as the gene

responsible for Rett syndrome (MIM 312750), which is a female-specific neurological disorder that manifests severe intellectual disability, seizures, and autistic features.¹ The *MECP2* mutations identified in typical female patients with

received
September 19, 2014
accepted
September 23, 2014

Issue Theme Epilepsy in Numerical Chromosomal Abnormalities; Guest Editor: Toshiyuki Yamamoto, MD, PhD

Copyright © 2015 by Georg Thieme Verlag KG, Stuttgart · New York

DOI <http://dx.doi.org/10.1055/s-0035-1554789>.
ISSN 2146-457X.

Rett syndrome have yet to be found in male patients, suggesting male lethality and X-linked dominant effects.² Nevertheless, the unique *MECP2* mutations have been identified in male patients with nonspecific intellectual disability.³ This indicates that *MECP2* mutations may have different genetic mechanisms and different clinical impacts in male and female patients, respectively.

Compared with mutations in *MECP2*, genomic copy number gains of *MECP2* are associated with entirely different clinical manifestations. In 2005, chromosomal duplications of Xq28, including *MECP2*, were identified in male patients with severe neurological impairments; this clinical presentation has previously been recognized as the Lubs-type X-linked mental retardation syndrome (MIM 300260).⁴ This condition, now known as the *MECP2* duplication syndrome, inherits as an X-linked recessive trait, and most of the patients' mothers having Xq28 duplications are nonmanifesting carriers.⁵ Male patients with Xq28 duplications including *MECP2* show early developmental delay during infancy.⁶ In addition, patients begin to present symptoms such as seizures and progressive deterioration in accordance with their growth. In most of the cases, seizures are intractable and refractory.

Here, we review patients with Xq28 duplications who manifest epilepsy and review the association between the symptoms and duplication size.

Variable Patterns of Xq28 Duplications

Xq28 duplications are the most frequently observed chromosomal duplications in patients with intellectual

disability of unknown etiology.⁷ These duplications occur by variable mechanisms, including interstitial duplications mediated by segmental duplications in this region as well as terminal duplications derived from translocation with other chromosomes. The most commonly observed pattern is the interstitial duplication that includes *MECP2*, which is due to regional genomic instability caused by segmental duplications that are densely located in this region. Variation in the sizes of the interstitial duplications is dependent on the breakpoints brought about by nonallelic homologous recombination. Therefore, some patients with *MECP2* duplications have larger duplications with expanded genomic regions. In such cases, the neighboring genes, such as the GDP dissociation inhibitor 1 (*GDI1*) gene and the inhibitor of kappa light polypeptide gene enhancer in B-cells, kinase gamma (*IKBKG*) gene, are included in the duplicated segment (→ Fig. 1).

GDI1 is related to X-chromosome inactivation and its loss-of-function mutations cause nonspecific intellectual disability.⁸ Moreover, duplications of *GDI1* alone result in moderate intellectual disability and microcephaly.⁹ Therefore, combined duplications with *MECP2* and *GDI1* may show more severe manifestations.

Incidence of Epilepsy in Xq28 Duplications

In 2005, Van Esch et al¹⁰ identified Xq28 duplications, including *MECP2*, as a frequent cause of severe intellectual disability and progressive neurological symptoms in males. They identified four large families with Xq28 duplications and

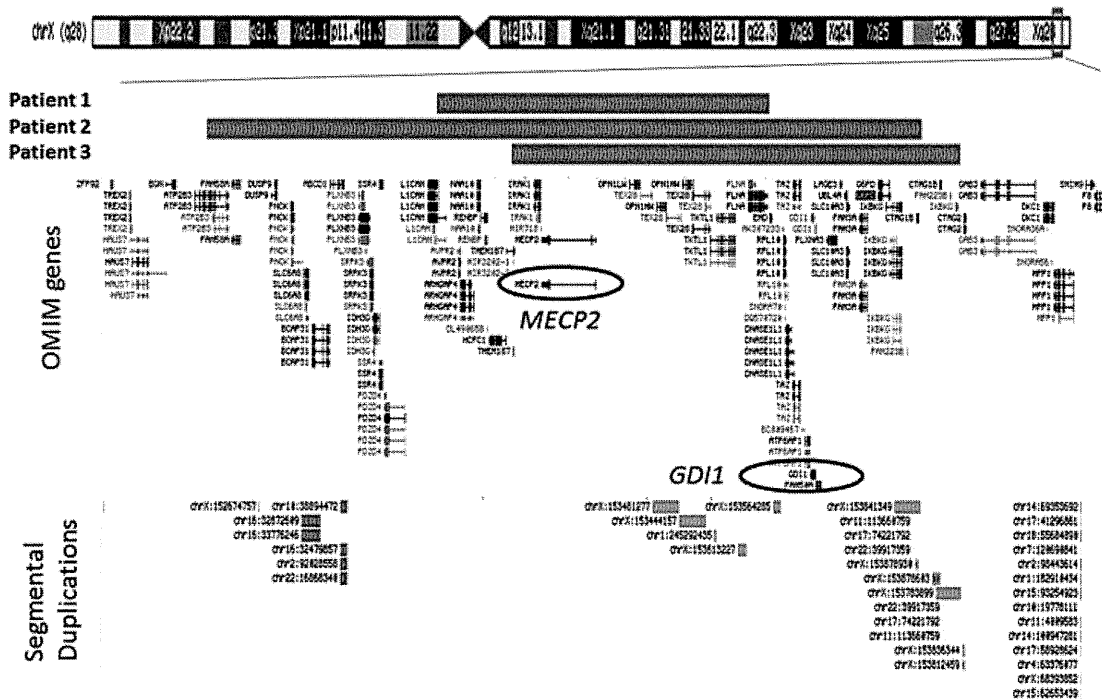


Fig. 1 The genome map around Xq28 region. Schematic representation and the genome map are downloaded from the University of California, Santa Cruz Genome Browser (<https://genome.ucsc.edu/>). *MECP2* is included in the minimum duplication region among three patient, whereas *GDI1* is included in the duplicated regions in patients 2 and 3. There are many segmental duplications in this region.

analyzed the clinical data of affected patients. The result showed that the frequency of seizures was 44% (4/9). In addition, Meins et al⁴ identified a patient with an *MECP2* duplication that has a minimum size and limited to the *MECP2* region. This patient started to show generalized epilepsy with absences, as well as myotonic-astatic and tonic seizures. The electroencephalogram (EEG) showed hypersynchronous activity and a very slow basal rhythm in the EEG of the awake state. Furthermore, Friez et al¹¹ identified six families with Xq28 duplications and analyzed the clinical features of the patients. It was found that the frequency of seizures was 65% (15/23). Therefore, the authors of this report concluded that no specific EEG patterns associated with the cases can be identified. In addition, Echenne et al¹² reported five patients from two families harboring minimum sizes of Xq28 duplications, including *MECP2*. Among them, three of the patients (3/5) showed epilepsy, which started at 8 to 19 years of age. Another similar study was also performed by Ramocki et al,¹³ in which eight families with Xq28 duplications were analyzed, and results demonstrated that epilepsy was observed in four out of nine patients (4/9). The authors reviewed the incidence of epilepsy in 110 previously reported patients, in which 52% of the patients showed epilepsy. However, these analyses did not take into account the age of the patients at the point of examination and patients from different age brackets were included.

Vignoli et al¹⁴ reported eight unrelated patients with *MECP2* duplications. Among them, all patients age over 10 years showed seizures; the results found that the ages of seizure onset were between 9 and 24 years. Therefore, it was concluded that the variability in seizure incidence found in different studies depends on the age of the patient at the time of recruitment. They further mentioned that seizure onset in early childhood before 3 years is a rare event (5/41, 12%). Fukushi et al¹⁵ reported a family consisting of five affected male patients with typical *MECP2* duplications, who started to show seizures between the ages 6 and 12 years. Furthermore, Caumes et al¹⁶ reported eight patients with *MECP2* duplications, who started to have seizures at a median age of 6 years (range: 2.5–17 years); half of these patients exhibited late-onset epileptic spasms, while the other demonstrated either focal epilepsy or unclassified generalized epilepsy. However, no unique EEG pattern was found.

As described above, patients generally begin to show epilepsy after 6 years of age. Therefore, incidence of epilepsy is highest in adolescents.

Seizure Types in Patients with Xq28 Duplications

Van Esch et al¹⁰ described four families with *MECP2* duplications. In one of the families, absence seizures were observed in a patient (L36; IV-1) since 2 years of age, whereas generalized tonic-clonic seizures were observed in another patient (L36; III-4) since 24 years of age, indicating clinical heterogeneity. Although the duplication was large in a family (T33) and included *GDI1* in the duplicated region, the affected patients in this family show no epilepsy.

Friez et al¹¹ reported six families with *MECP2* duplications. Seizure types and ages of onset were varied in patients with atonic seizures that began at 7 years (K8315; II-2), myoclonic seizures that began at 9 years (K9227; III-6), and complex partial seizures at 5 years (K9228; II-2). It is noticeable that one patient (K9244; II-3) started to show seizures from 6 months of age. Smyk et al¹⁷ reported three male patients with *MECP2* duplications; one of them developed recurrent tonic-clonic seizures at 9 years of age. Five patients reported by Echenne et al¹² were from two families with a minimum size of Xq28 duplication, including *MECP2*. Three patients started to show epilepsy at 8 to 19 years of age. Seizure types included atypical absence, grand mal, generalized tonic-clonic, partial motor, myoclonic, and myoclonic-astatic seizures. Their EEG patterns were generalized and sometimes presented focalized theta and delta waves. Spike waves were rare and polyspike-wave activity was absent.

As described above, many types of epilepsy have been reported in patients. The most frequently described seizure types were absence seizure and generalized tonic-clonic seizures. Descriptions of drop attacks were also frequently seen. In comparison, focal seizures and complex partial seizures are relatively rare. This indicates generalized seizures are the main type of epilepsy. Patients easily lose consciousness during such attacks and often fall onto the ground. Therefore, the patient's safety can be seriously impaired during daily drug-resistant seizures when atonic seizures or drop attacks occur, and such epileptic attacks cause injuries that are sometimes life-threatening.¹⁴

In a previous report, drug resistance was found in almost half of published results. Caumes et al¹⁶ described that half of the patients show late-onset epileptic spasms, while 75% of the patients had refractory epilepsy.

Case Presentation

Here, we demonstrate three unrelated patients with *MECP2* duplications.

Patient 1

A 17-year-old boy was previously reported as patient 2 by us.⁵ Initially, he was diagnosed as having autism of unknown etiology, because he showed developmental delay and autistic features from his infancy. When he was 13-year-old, he started to show epileptic seizures. Various types of seizures have been observed, including drop attacks and generalized tonic-clonic seizures. The frequencies of these seizure attacks increased gradually. The drop attacks were life-threatening and he frequently injured his tongue. EEG showed generalized theta wave activity associated with polyspikes (► Fig. 2A). At present, combinatory use of antiepileptic drugs, including 1,000 mg of valproic acid (VPA), 700 mg of ethosuximide (ESM), 300 mg of topiramate, and 100 mg of lamotrigine, is administered, but his seizures are still intractable. Microarray-based comparative hybridization analysis identified an Xq28 duplication which contained *MECP2* but not *GDI1* (► Fig. 1).

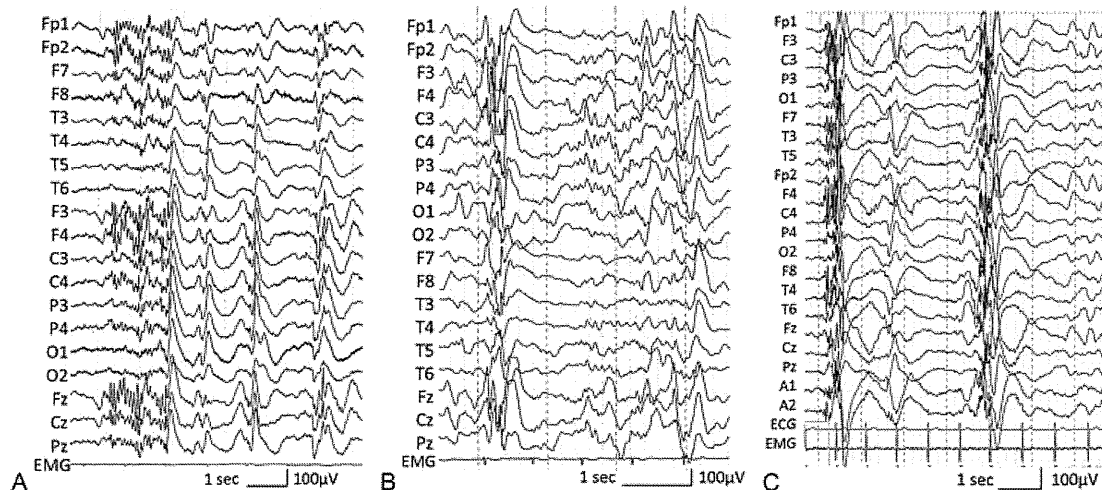


Fig. 2 Electroencephalogram (EEG) findings of the present patients. (A) Sleep EEG of patient 1. Front-central dominant theta bursts associated with polyspikes and waves are noted. (B) Sleep EEG of patient 2. Front-central dominant polyspikes and waves are shown. (C) Sleep EEG of patient 3. Periodic appearance of polyspikes and theta wave complexes is noted.

Patient 2

A 7-year-old boy who was previously reported by us as patient 5 showed poor sucking and recurrent vomiting since his early infancy.⁷ Early developmental delay and axial hypotonia were also noted. He was frequently admitted to the hospital due to recurrent pneumonia. Since the age of 1 year, he began having daily spasms with flexion of both the arms. After prescription of VPA, the frequency of the spasms decreased. Although he had been able to sit alone and eat independently, poor oral intake and swallowing difficulty started to show after the inception of drop attacks since the age of 4 years. Subsequently, he lost the ability to sit alone by himself. Phenobarbital, zonisamide, clonazepam, and ESM were administered but the frequency of the myoclonic spasms was gradually increased. At present, he shows partial seizures associated with extension of his upper extremities and series of epileptic spasms. Now, he is prescribed with VPA, ESM, and also lamotrigine. EEG demonstrated front-central dominant polyspikes and waves (→Fig. 2B). This patient harbors chromosomal duplication involving *MECP2* and *GDI1* (→Fig. 1).

Patient 3

A 14-year-old boy, who was previously reported by us as patient 11, was born at 36 weeks of gestation.⁷ His birth weight was 2,294 g (<3rd percentile), length was 48 cm (25–50th percentile), and occipitofrontal circumference was 32 cm (10–25th percentile). He showed developmental delay since early infancy; he could only walk independently at 18 months. During his early infancy, there were many occurrences of infection. When he was 10-year-old, he suffered myoclonic seizures. Thereafter, clustering of epileptic spasms and myoclonic twitches were observed. These seizures were intractable against VPA, levetiracetam, and clorazepate dipotassium. EEG demonstrated periodic appearance of polyspikes and theta wave complexes (→Fig. 2C). At present, his height is 165 cm (50–75th percentile), weight is 60 kg

(75–90th percentile), and occipitofrontal circumference of 60 cm (>97th percentile), indicating macrocephaly. He shows distinctive features, including frontal bossing and thick vermilions. Microarray-based comparative hybridization analysis identified an Xq28 microduplication, including *MECP2* and *GDI1* (→Fig. 1).

Genotype–Phenotype Correlation Regarding Epilepsy in Xq28 Duplication

Patients 1 and 3 described above showed typical clinical course for the *MECP2* duplication syndrome. In contrast, patient 2 showed severe epileptic features with epileptic spasms in infancy. Because patient 2 showed larger duplication in the *MECP2* region and that included *GDI1*, we suspected that the additional duplication of *GDI1* may exert an effect in this case. However, patient 3 also showed combinatory duplication with *MECP2* and *GDI1*, same as patient 2. To analyze the impacts of the additional *GDI1* duplication, we conducted a comprehensive review of previously reported patients with combined duplications with *MECP2* and *GDI1*.

Clayton-Smith et al¹⁸ reported 10 families affected with Xq28 duplications including *MECP2*. Among them, three families (Family 3, 6, and 10) showed larger duplications, which included *GDI1* in the duplicated regions. The probands in family 3 showed recurrent respiratory problems and died in infancy consequently. The proband in family 6 showed severe delay in development and epilepsy from his early infancy; however, detailed information regarding this manifestation is unavailable. The proband in family 10 showed seizure disorder, which began at the age of 13 years.

Lugtenberg et al¹⁹ reported six families with Xq28 duplications including *MECP2*. Among them, one family (Family F) showed inclusion of *GDI1* in the duplicated region. One of the probands showed typical phenotypic features of *MECP2* duplication syndrome and manifested epilepsy that started

at the age of 8 years. The other proband showed no epilepsy until the age of 6 years.

Reardon et al²⁰ reported three families with Xq28 duplications, which included both of *MECP2* and *GDI1*. There were seven affected males in the families. Among them, four patients showed epilepsy, which began to manifest between the ages of 4 and 7 years.

Despite comprehensive review of the literature, we were not able to obtain all of the detailed genotypes of the reported patients, and the information we did acquire as described above was limited. However, the majority of patients with combined duplications with *MECP2* and *GDI1* show similar courses of epilepsy as patients having the typical *MECP2* duplications. Therefore, we could not demonstrate that the severity of epilepsy is affected by larger duplications that include *GDI1*. Further information would be required to confirm genotype–phenotype correlation for the *MECP2* duplication syndrome.

Acknowledgments

We would like to express our gratitude to the patients and their families for their cooperation. This work was supported by a Grant-in-Aid for Scientific Research from Health Labor Sciences Research Grants from the Ministry of Health, Labor, and Welfare, Japan (T. Y.).

References

- Amir RE, Van den Veyver IB, Wan M, Tran CQ, Francke U, Zoghbi HY. Rett syndrome is caused by mutations in X-linked *MECP2*, encoding methyl-CpG-binding protein 2. *Nat Genet* 1999;23(2):185–188
- Philippe C, Villard L, De Roux N, et al. Spectrum and distribution of *MECP2* mutations in 424 Rett syndrome patients: a molecular update. *Eur J Med Genet* 2006;49(1):9–18
- Villard L. *MECP2* mutations in males. *J Med Genet* 2007;44(7):417–423
- Meins M, Lehmann J, Gerresheim F, et al. Submicroscopic duplication in Xq28 causes increased expression of the *MECP2* gene in a boy with severe mental retardation and features of Rett syndrome. *J Med Genet* 2005;42(2):e12
- Shimada S, Okamoto N, Ito M, et al. *MECP2* duplication syndrome in both genders. *Brain Dev* 2013;35(5):411–419
- Ramocki MB, Tavyev YJ, Peters SU. The *MECP2* duplication syndrome. *Am J Med Genet A* 2010;152A(5):1079–1088
- Yamamoto T, Shimojima K, Shimada S, et al. Clinical impacts of genomic copy number gains at Xq28. *Human Genome Variation*. Available at: <http://www.nature.com/articles/hgv20141>. Accessed September 19, 2014
- Bienvenu T, des Portes V, Saint Martin A, et al. Non-specific X-linked semidominant mental retardation by mutations in a Rab GDP-dissociation inhibitor. *Hum Mol Genet* 1998;7(8):1311–1315
- Vandewalle J, Van Esch H, Govaerts K, et al. Dosage-dependent severity of the phenotype in patients with mental retardation due to a recurrent copy-number gain at Xq28 mediated by an unusual recombination. *Am J Hum Genet* 2009;85(6):809–822
- Van Esch H, Bauters M, Ignatius J, et al. Duplication of the *MECP2* region is a frequent cause of severe mental retardation and progressive neurological symptoms in males. *Am J Hum Genet* 2005;77(3):442–453
- Friez MJ, Jones JR, Clarkson K, et al. Recurrent infections, hypotonia, and mental retardation caused by duplication of *MECP2* and adjacent region in Xq28. *Pediatrics* 2006;118(6):e1687–e1695
- Echenne B, Roubertie A, Lugtenberg D, et al. Neurologic aspects of *MECP2* gene duplication in male patients. *Pediatr Neurol* 2009;41(3):187–191
- Ramocki MB, Peters SU, Tavyev YJ, et al. Autism and other neuropsychiatric symptoms are prevalent in individuals with *MeCP2* duplication syndrome. *Ann Neurol* 2009;66(6):771–782
- Vignoli A, Borgatti R, Peron A, et al. Electroclinical pattern in *MECP2* duplication syndrome: eight new reported cases and review of literature. *Epilepsia* 2012;53(7):1146–1155
- Fukushi D, Yamada K, Nomura N, et al. Clinical characterization and identification of duplication breakpoints in a Japanese family with Xq28 duplication syndrome including *MECP2*. *Am J Med Genet A* 2014;164A(4):924–933
- Caumes R, Boespflug-Tanguy O, Villeneuve N, et al. Late onset epileptic spasms is frequent in *MECP2* gene duplication: electroclinical features and long-term follow-up of 8 epilepsy patients. *Eur J Paediatr Neurol* 2014;18(4):475–481
- Smyk M, Obersztyn E, Nowakowska B, et al. Different-sized duplications of Xq28, including *MECP2*, in three males with mental retardation, absent or delayed speech, and recurrent infections. *Am J Med Genet B Neuropsychiatr Genet* 2008;147B(6):799–806
- Clayton-Smith J, Walters S, Hobson E, et al. Xq28 duplication presenting with intestinal and bladder dysfunction and a distinctive facial appearance. *Eur J Hum Genet* 2009;17(4):434–443
- Lugtenberg D, Kleefstra T, Oudakker AR, et al. Structural variation in Xq28: *MECP2* duplications in 1% of patients with unexplained XLMR and in 2% of male patients with severe encephalopathy. *Eur J Hum Genet* 2009;17(4):444–453
- Reardon W, Donoghue V, Murphy AM, et al. Progressive cerebellar degenerative changes in the severe mental retardation syndrome caused by duplication of *MECP2* and adjacent loci on Xq28. *Eur J Pediatr* 2010;169(8):941–949

